Journal of Applied Electrochemistry (2005) 35:85–90
DOI 10.1007/s10800-004-4059-9

Characterization of different Pt/Metal/Complex catalysts as anode catalysts for the PEM fuel cell

N. MARTZ*, C. ROTH and H. FUEß
University of Darmstadt, Institute of Materials Science, Petersenstrasse 23, D-64287 Darmstadt, Germany
*(*author for correspondence, e-mail: martz@st.tu-darmstadt.de)*

Received 24 March 2003; accepted in revised form 16 August 2004

Key words: BET, chelate, DMFC, EDXS, PEMFC, platinum, TEM, XRD

Abstract

Different Pt/Me/Pc and Pt/Me/Complex catalysts (with Me = Metal: Co, Ni, and Pc = phthalocyanine) were synthesized by an impregnation method. A commercially available platinum catalyst purchased from E-TEK. was impregnated with solutions of cobalt phthalocyanine (CoPc) and nickel phthalocyanine tetrasulfonic salt (NiPc). After the reaction, part of the catalyst was heat treated at 700 °C under nitrogen atmosphere. The resulting catalysts were structurally and electrochemically characterized before (Pt/Me/Pc) and after heat treatment (Pt/Me/Complex). The Pt/Me/Pc had an average particle size of about 3 nm, while the average size after heat treatment increased to about 7 nm. The composition of the different catalysts was about 80 at% platinum and 20 at% of the second metal (Co or Ni), and was verified with EDXS. In single fuel cell tests the best electrocatalytic activity was observed for the Pt/Ni/Complex system.

1. Introduction

To reduce costs, it is desirable to run fuel cells with reformate gas or methanol instead of expensive pure hydrogen. When such substitute fuels are used, carbon monoxide is produced blocking the electrocatalytic active platinum sites (CO poisoning [1]). This results in a decrease in cell potential. The addition of other (transition) metals to the catalyst reduces the CO poisoning effect. A binary Pt/Ru system which significantly improves the performance for the anodic oxidation of reformate gas and methanol has already been commercially applied. Consequently numerous investigations of the Pt/Ru system have been reported [2–7]. Ternary systems like Pt/Ru/W, Pt/Ru/Sn and Pt/Ru/Mo [8–12] show even higher activities than binary Pt/Ru catalysts. However, expensive noble metals are still needed for good performance.

A promising approach towards higher electrode activity is the application of macrocycles in order to stabilize non-noble transition elements (e.g., Fe, Co, Rh, Sn and Ni) at working conditions in an acidic environment. These complexes may be used in combination with standard platinum catalysts. Bett et al. [13] investigated phthalocyanine complexes of iron, cobalt, nickel and tin, as well as ruthenium tetramethylcyclam as co-catalysts for anodic methanol oxidation. A co-catalytic activity was reported for tin phthalocyanine, the activity of this catalyst being smaller than the activity of a commercial Pt/Ru catalyst but higher than for pure platinum. The activity of different macrocyclic transition metal complexes in acidic solution was also studied by Jahnke et al. [14]. For cobalttetraazaannulene only activity for the anodic oxidation of formic acid and hydrazine was found, in addition to a very low activity for the anodic oxidation of carbon monoxide. Van Veen et al. and van Baar et al. [15, 16] reported carbon-supported rhodium and iridium porphines to be highly active for the anodic oxidation of carbon monoxide in acidic electrolytes. In both cases enhanced activity was observed after pyrolysis of the complexes at 700 °C under nitrogen [17]. From electrochemical experiments it is inferred that the metals are still present in an oxidized state after heat treatment. The authors propose a catalytically active centre consisting of the central ion with its surrounding ring of nitrogen ligands which is fused to the carbon surface by pyrolysis of the complex.

In the present work, the structure and electrocatalytic activity of differently synthesized catalysts are studied to improve an understanding of the relation between the catalyst structures and their electrocatalytic properties. The structural characterization of the different catalysts was carried out by BET, X-ray diffraction (XRD), transmission electron microscopy (TEM) and nano-energy dispersive spectroscopy (nano-EDXS). Single fuel cell tests were performed for the electrochemical characterization.

2. Experimental details

2.1. *Preparation of Pt/Me/Pc and Pt/Me/Complex catalysts (with Me = Co and Ni)*

Carbon black (Vulcan XC-72, Cabot International) with a specific surface area (BET) of 290 m^2 g^{-1} was used as support for all catalysts. A commercial carbon-supported platinum catalyst was purchased from E-TEK. (Natick, MA, USA) with a metal loading of 20 wt% platinum on Vulcan XC-72. Cobalt phthalocyanine (CoPc) and nickel phthalocyanine tetrasulfonic salt (NiPc) were purchased from Aldrich; schemes of the chelates are shown in Figure 1.

The chelate complexes described above were dissolved in appropriate solvents at 80 °C and slowly added to a suspension of the carbon-supported platinum catalyst (E-TEK) in the same solvent which had been previously treated for 15 min in an ultrasonic bath. A stoichiometric amount of 80 at% platinum and 20 at% of the second metal was used for the synthesis. The mixture was boiled for 3 h under reflux and the solvent was removed by distillation, resulting in the Pt/Me/Pc (with Me = Co and Ni) catalyst. Part of the Pt/Me/Pc catalysts was heat treated at 700 °C under nitrogen to enhance the electrocatalytic activity [17]. Heat-treated systems that follow are denoted Pt/Me/Complex catalysts (with Me = Co and Ni).

2.2. *Electrochemical measurements*

For the electrochemical investigation of the various catalysts, single cell experiments using pure hydrogen, reformate gas and methanol as anode feed were chosen to determine the electrocatalytic activity. Membrane electrode assemblies (MEAs) were manufactured by a spraying technique, as described by Wilson and Gottesfeld [18]. In all cases, a commercially available platinum system (20 wt% on Vulcan, E-TEK) was used as cathode sprayed onto a standard perfluorosulphonic acid membrane (Nafion® 117 by DuPont). The as-synthesized and heat-treated macrocycle catalysts were applied on the anode side yielding an active MEA area of 25 cm^2. The single cell was operated under standard conditions at 75 °C with pure hydrogen and reformate gas and at 95 °C with vapourized 1 M aqueous methanol/water solution, respectively.

Current–potential (*E*/*i*) curves were recorded for pure H_2, H_2/CO mixtures with CO concentrations of 75 ppm and 150 ppm and in methanol operation. The different Pt/Me/Pc and Pt/Me/Complex catalysts were compared to the commercial platinum catalyst.

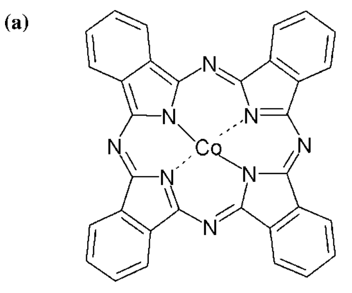

Cobalt phthalocyanine (CoPc)

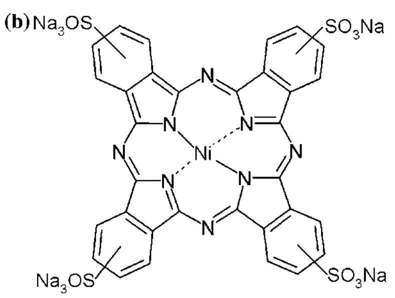

Nickel phthalocyanine tetrasulfonic salt (NiPc)

Fig. 1. Scheme of the chelate complexes: (a) CoPc and (b) NiPc.

2.3. *Structural characterization*

The catalysts were analysed by transmission electron microscopy using a Philips CM 20 UT with an acceleration voltage of 200 kV and a tungsten filament. An EDXS unit with Ge detector connected to the microscope was used to study the composition of individual nanoparticles. TEM samples were prepared by suspending the catalyst powder in anhydrous methanol and depositing a drop of the suspension on a standard carbon-covered copper grid. The particle measurement was performed with the program package LINCE [19] and the particle size distributions calculated accordingly.

A STOE STADI-P with germanium monochromatized CoK_α radiation and a position sensitive detector with 6° aperture in transmission mode was used for X-ray powder diffraction. Rietveld refinement was carried out to obtain average particle sizes using the FULLPROF software [20].

3. Results and discussion

3.1. *BET measurements*

BET isotherms were measured using nitrogen physisorption, and the specific surface areas of the different carbon-supported catalysts were determined (Table 1).

Table 1. BET measurements

	S /m^2 g^{-1}
Pt/Co/Pc	52.81
Pt/Ni/Pc	41.38
Pt/Co/Complex	88.85
Pt/Ni/Complex	75.76
Pt E-TEK	167.7

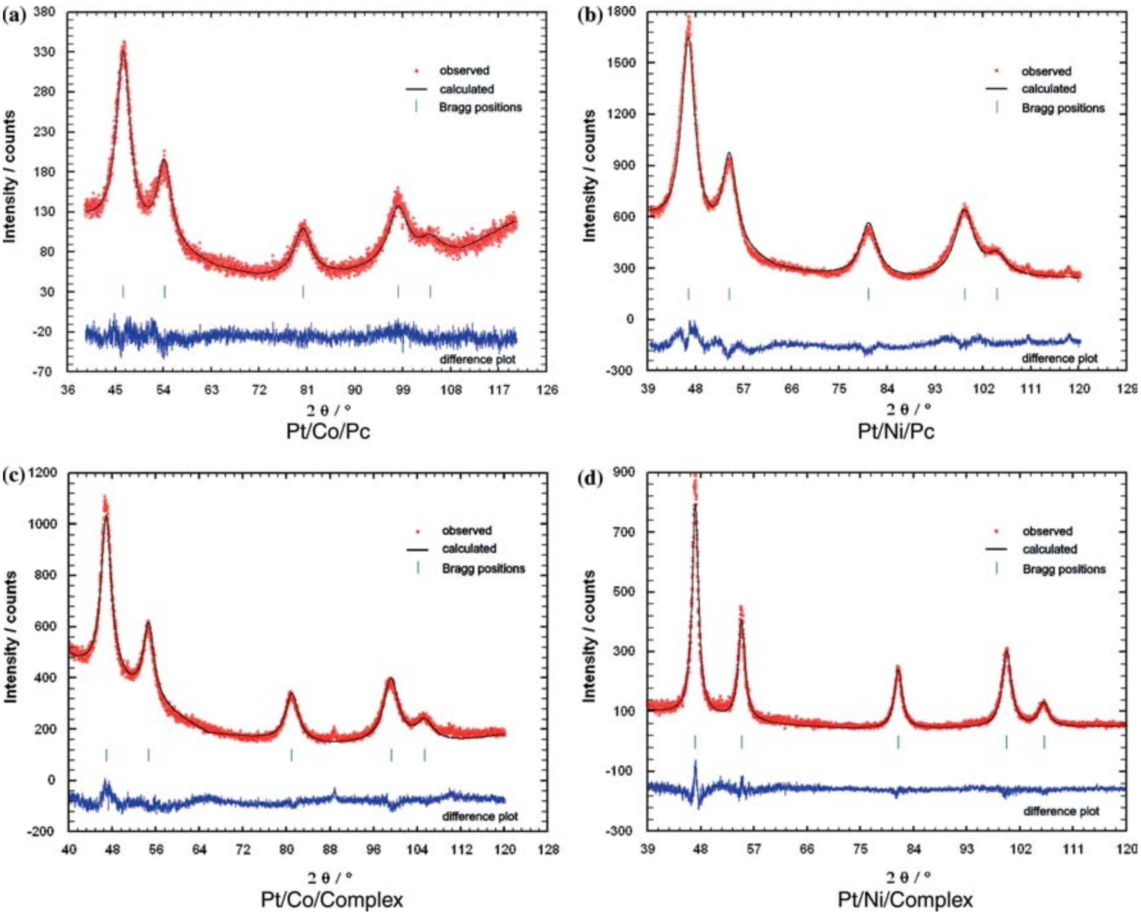

Fig. 2. Powder patterns of (a) Pt/Co/Pc, (b) Pt/Ni/Pc, (c) Pt/Co/Complex and (d) Pt/Ni/complex catalysts; the Rietveld refinement plot is shown, black line = calculated pattern, red line = observed pattern, and blue line = difference plot.

The specific surface area of the in-house synthesized catalysts is smaller than that of the commercial platinum catalyst. This is probably due to the complexes covering the active catalyst surface. In addition, an increase in the specific surface area is observed for the catalysts after heat treatment. It is assumed that part of the complex is burned at higher temperatures, thereby exposing additional support surface.

3.2. *X-ray diffraction (XRD)*

X-ray diffraction was performed on the as-synthesized Pt/Me/Pc, Pt/Me/Complex systems and the platinum catalyst. The patterns shown in Figure 2 exhibit the characteristic reflections of the platinum f.c.c. structure with no evidence of additional phases. The average particle sizes determined are listed in Table 2. The as-synthesized systems show the same behaviour as the commercial platinum system. Due to the heat treatment at 700 °C under nitrogen atmosphere an increase from 2–3 nm to 4–5 nm in particle size was observed.

Table 2. Average particle sizes as determined by XRD and TEM

	XRD particle size / nm	TEM particle size /nm
Pt/Co/Pc	2.0	3.75 ± 0.77
Pt/Ni/Pc	2.3	3.19 ± 0.72
Pt/Co/Complex	3.1	5.84 ± 1.85
Pt/Ni/Complex	5.6	6.38 ± 2.02
Pt E-TEK	1.9	3.11 ± 0.99

3.3. *Transmission electron microscopy (TEM)*

Figure 3 shows electron micrographs of the different Pt/Me/Pc and Pt/Me/Complex catalysts. The images show homogeneously dispersed nanocrystals on the edges of each micrometer-sized carbon support grain, and closely resemble those of the commercially available platinum catalyst. For the different samples, the particle sizes were measured and the particle size distributions determined (Figure 4). From the particle size distributions the average particle sizes were calculated and the results summarized in Table 2.

The particle sizes obtained are in good agreement with the XRD results. The average particle size increases significantly after heat treatment at 700 °C in nitrogen atmosphere. This is in contrast to recent investigations of Bönnemann et al. [21] who observed only small particle growth under nitrogen flow.

In addition to the electron micrographs depicted in Figure 3 high resolution TEM (HRTEM) images were

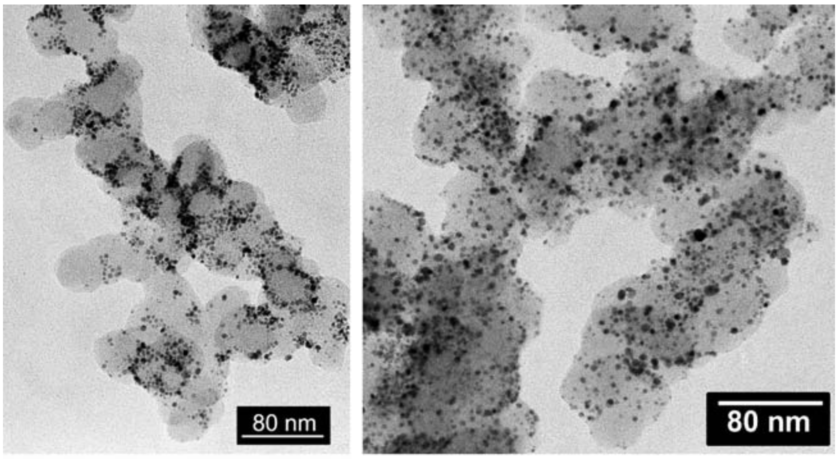

(a) Pt/Co/Pc

(b) Pt/Ni/Pc

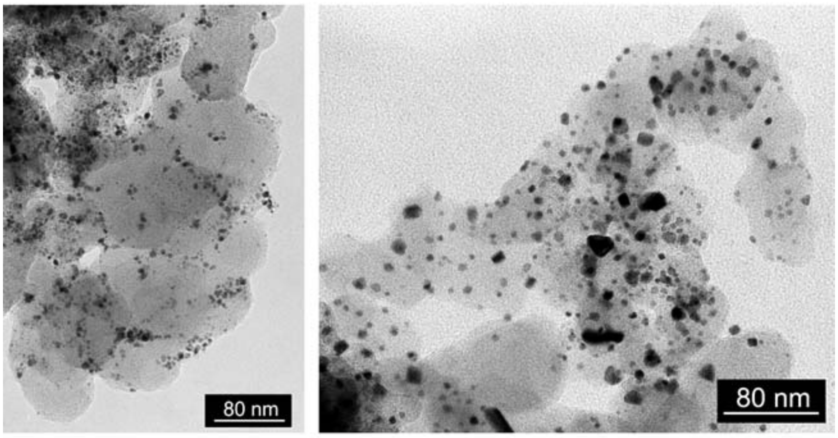

(c) Pt/Co/Complex

(d) Pt/Ni/Complex

Fig. 3. TEM images of (a) Pt/Co/Pc, (b) Pt/Ni/Pc, (c) Pt/Co/Complex and (d) Pt/Ni/Complex.

recorded. In the HRTEM mode lattice planes of distinct nanoparticles can be imaged thus allowing an accurate measurement of d spacings. Two different d values were found, $d = 1.99$ Å corresponding to Pt (200) and $d = 2.27$ Å attributed to Pt (111).

3.4. *Nano-energy dispersive spectroscopy (nano-EDXS)*

Nano-EDXS enables determination of the composition of individual particles. Figure 5 shows the compositional distribution obtained by the EDXS measurements of the as-synthesized and the heat-treated catalysts. 20 particles per sample were analysed and the deviation from the average composition was determined. The stoichiometric quantities employed for the synthesis are in good agreement with the measured compositions for the Pt/Ni/Pc and Pt/Ni/Complex catalyst. In contrast the as-synthesized and the heat-treated cobalt samples show significant deviations. This may be due to the TEM sample preparation in anhydrous methanol: the cobalt phthalocyanine might be 'leached' from the support, as it is more soluble in methanol than the corresponding Ni macrocycle.

3.5. *Current–potential curves*

The electrocatalytic activities of the respective catalyst materials were measured in single cells with pure hydrogen, reformate gas and methanol under normal pressure. In Figure 6, E/i curves are shown for the different catalysts in different operation modes. For a better comparison, the electrocatalytic activity was measured as the current density i at 600 mV (400 mV for methanol) normalized to the same current density in pure hydrogen operation. The values obtained are listed in Table 3. Apart from the as-synthesized Pt/Ni/Pc, all other macrocycle catalysts show higher activities than plain platinum. In agreement with van Veen et al. [17] a significant improvement in activity is found after heat treatment.

4. Conclusion

Various Pt/Me/Complex catalysts (with Me = Co and Ni) were synthesized by an impregnation method using a commercial platinum catalyst from E-TEK as precursor. The system nanostructure was characterized using

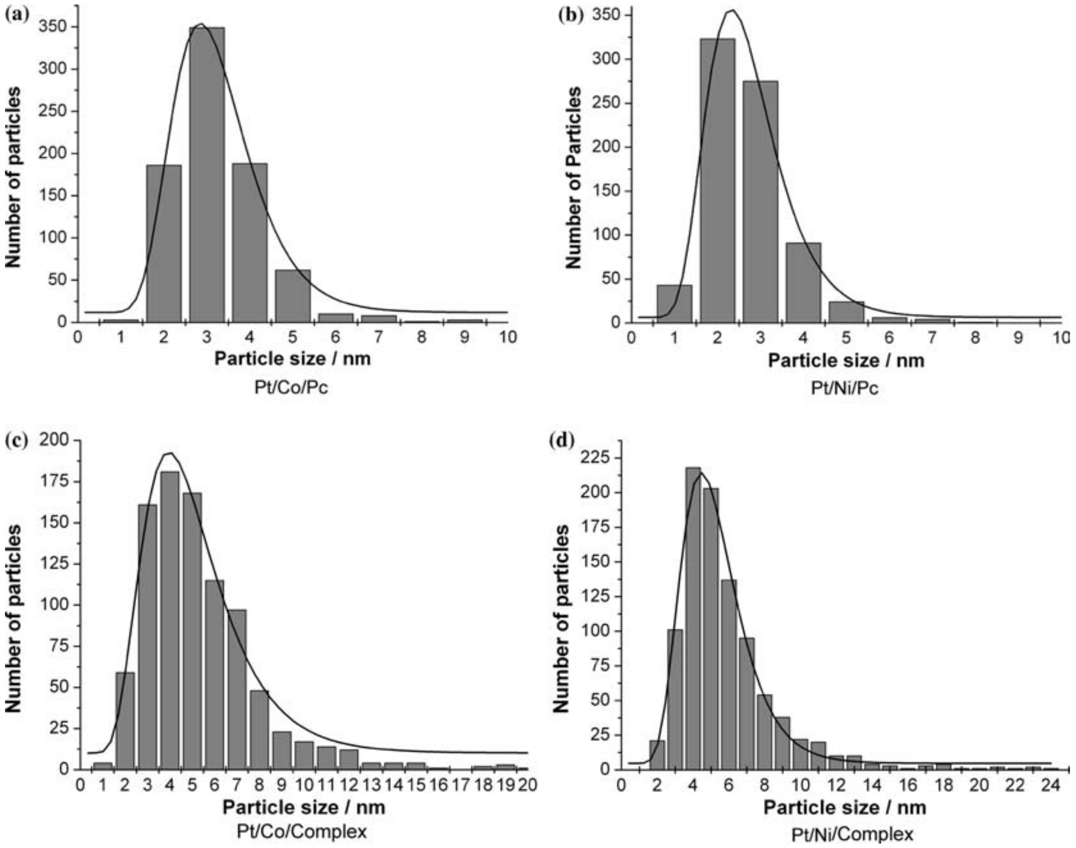

Fig. 4. Particle size distributions of (a) Pt/Co/Pc, (b) Pt/Ni/Pc, (c) Pt/Co/Complex and (d) Pt/Ni/Complex.

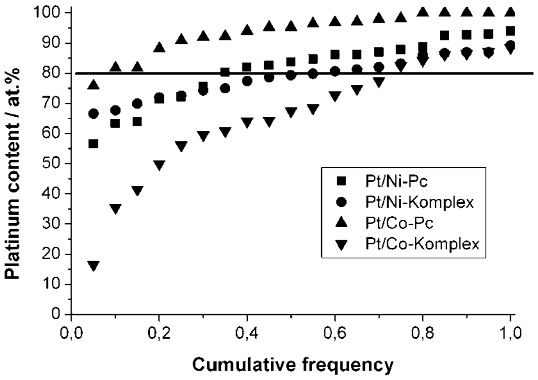

Fig. 5. Composition of individual nanoparticles as determined by nano-EDXS; measured for Pt/Co/Pc, Pt/Ni/Pc, Pt/Co/Complex and Pt/Ni/Complex.

BET, XRD, TEM and nano-EDXS before and after heat treatment. The electrocatalytic activity was evaluated by current–voltage curves in a fuel cell operating with hydrogen, H_2/CO and methanol.

TEM images show highly-dispersed nanocrystals for all samples differing merely in the measured particle sizes. The Pt/Me/Pc exhibit an average particle size of about 3 nm which increases up to 7 nm during heat treatment. The average particle sizes determined by Rietveld refinement of the X-ray patterns are in good agreement with the sizes determined by TEM. Only slightly larger particles were found in the TEM images due to the additional non-coherent scattering contribution.

By nano-EDXS the composition of individual nanoparticles was determined showing good agreement between the measured values and the quantities employed for the catalyst syntheses (i.e., about 80 at% of platinum and 20 at% of the second metal).

The electrocatalytic activity of the catalysts was measured in single cells yielding activities better than pure platinum. Heat treatment at 700 °C under nitrogen atmosphere leads to an enhancement of the electrocatalytic activity according to results reported previously by van Veen et al. [17].

Acknowledgement

Support of this work by the Deutsche Forschungsgemeinschaft and the Fonds der Chemischen Industrie is gratefully acknowledged. Thanks are due to Frank Haass, TU Darmstadt, for the BET measurements.

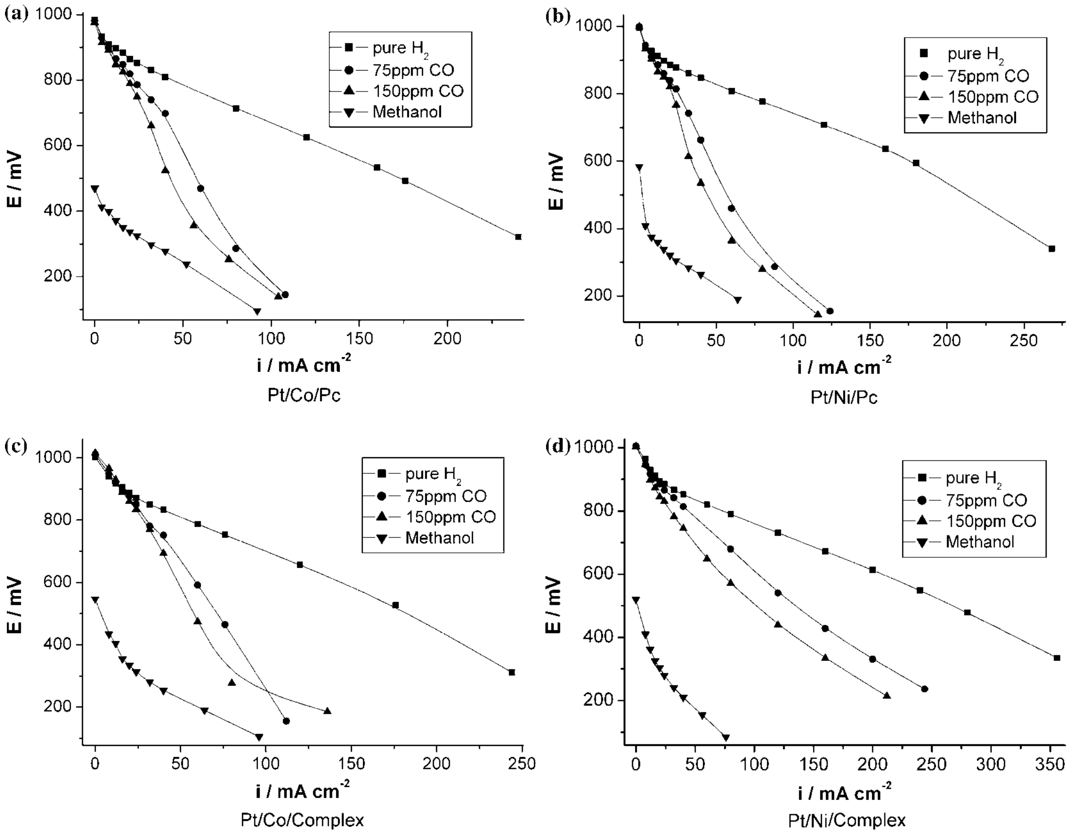

Fig. 6. *E*/*i* curves for (a) Pt/Co/Pc, (b) Pt/Ni/Pc, (c) Pt/Co/Complex and (d) Pt/Ni/Complex. Key: (■) pure H_2, (●) 75 ppm CO, (▲) 150 ppm CO and (▼) methanol.

Table 3. Current density at 600 mV (400 mV for methanol) normalized to the current density in hydrogen operation

	75 ppm CO / %	150 ppm CO / %	Methanol / %
Pt/Co/Pc	37	27	3
Pt/Ni/Pc	26	19	2
Pt/Co/Complex	41	33	5
Pt/Ni/Complex	50	35	3
Pt E-TEK	38	21	2

References

1. K. Kunimatsu, K. Schimazu and H. Kita, *J. Electroanal. Chem.* **256** (1988) 371.
2. H.A. Gasteiger, N.M. Markovic and P.N. Ross Jr, *J. Phys. Chem.* **98** (1994) 617.
3. H.A. Gasteiger, N.M. Markovic and P.N. Ross Jr, *J. Phys. Chem.* **99** (1995) 16757.
4. H.A. Gasteiger, N.M. Markovic and P.N. Ross Jr, *J. Phys. Chem.* **99** (1995) 8290.
5. A.S. Aricò, P. Creti, H. Kim, R. Mantegna, N. Giordano and V. Antonucci, *J. Electroanal. Chem.* **143** (1996) 3950.
6. H.-F. Oejten, V. Schmidt, U. Stimming and F. Trila, *J. Electrochem. Soc.* **143** (1996) 3838.
7. C. Roth, N. Martz and H. Fuess, *Phys. Chem. Chem. Phys.* **3** (2001) 315.
8. G. Meli, J.-M. Léger, C. Lamy and R. Durand, *J. Appl. Electrochem.* **31** (1993) 197.
9. M. Goetz and H. Wendt, *J. Appl. Electrochem.* **31** (2001) 811.
10. A. Lima, C. Coutanceau, J.-M. Léger and C. Lamy, *J. Appl. Electrochem.* **31** (2001) 379.
11. C Roth, M. Goetz and H. Fuess, *J. Appl. Electrochem.* **31** (2001) 793.
12. .J.-M. Léger, *J. Appl. Electrochem.* **31** (2001) 767.
13. J.S. Bett, H.R. Kunz, A.J. Aldykiewicz, J.M. Fenton, W.F. Bailey and D.V. McGrath, *Electrochim. Acta* **43** (1998) 3545.
14. H. Jahnke, M. Schoenborn and G. Zimmermann, Thieme Verlag, Stuttgart, (1973).
15. J.A.R. van Veen, J.F. van Baar, C.J. Kroese, J.G.F. Coolegem, N. de Wit and H.A. Colijn, *Ber. Bunsenges. Phys. Chem.* **85** (1981) 693.
16. J.F. van Baar, J.A.R. van Veen, J.M. van der Eijk, T.J. Peters and N. de Wit, *Electrochim. Acta* **27** (1982) 1315.
17. J.A.R. van Veen, J.F. van Baar and C.J. Kroese, *J. Chem. Soc. Faraday Trans. 1* **77** (1981) 2827.
18. M.S. Wilson and S. Gottesfeld, *J. Electrochem. Soc.* **139** (1992) L28.
19. S.L. dos Santos e Lucato, 'Lince v 2.31', TU Darmstadt, FB Materials Science, Ceramic Group (1998).
20. J. Rodriguez-Carvajal, Congress of the International Union of Crystallography (1990), p. 127.
21. H. Bönnemann, R. Brinkmann, P. Britz, U. Endruschat, R. Mörtel, U.A. Paulus, G.J. Feldmeyer, T.J. Schmidt, H.A. Gasteiger and R.J. Behm, *J. New Mater. Electrochem. Systems* **3** (2000) 199.